



Research article

## Three-dimensional Thai dessert printing: A preliminary study on Khanom Ar-Lua

Natthavika Chansri, Wachiraporn Yindee, Suttinee Pattamanawin, Thittikorn Phattanaphibul\*

Integrated Design and Manufacturing System Research Unit, Faculty of Engineering at Sriracha, Kasetsart University, Chonburi 20230, Thailand

### Article Info

#### Article history:

Received 5 September 2023

Revised 3 December 2023

Accepted 5 December 2023

Available online 31 December 2023

#### Keywords:

3D-printing,

Ar-Lua,

Extrusion,

Nozzle,

Thai dessert

### Abstract

**Importance of the work:** Thai desserts require a lot of time to form their exquisite shapes. Three-dimensional (3D) printing may improve this process.

**Objectives:** To investigate the possibility of applying 3D printing in the Thai dessert industry.

**Materials & Methods:** A printing substrate was prepared according to the ingredients for cooking “Khanom Ar-Lua”. An extrusion-based, 3D printing technique was applied to create specimens. In addition, a new mechanical extrusion system was constructed and tested for its dimensional controllability of the deposited substrate.

**Results:** The results of the printed substrate showed good raster width, including consistency and repeatability. There were problems with misalignment between printed layers and the long drying time after the shaping step.

**Main finding:** 3D printing technology showed potential for application in the Thai dessert industry to improve the processing time spent in the shaping step. Further study will investigate using a 3D scanner and reverse engineering technology to prepare digital records of the exquisite shapes of Thai desserts that cannot be easily generated using a computer-aided design package.

\* Corresponding author.

E-mail address: [thittikorn@eng.sru.ku.ac.th](mailto:thittikorn@eng.sru.ku.ac.th) (T. Phattanaphibul)

## Introduction

Three-dimensional printing (3DP) is a digital manufacturing technology that creates a physical object via additive manufacturing methodologies, usually layer by layer. Advancement in both material science and processing technology have enabled 3DP to be favorably considered for a wide variety of applications, including the aerospace (Joshi and Sheikh, 2015), construction (El-Sayegh et al., 2020), modern automotive (Tan et al., 2022), medical (Liaw and Guvendiren, 2017), jewelry (Yap and Yeong, 2014), fashion design (Vanderploeg et al., 2017), electronics (Park et al., 2022), and food industries (Nachal et al., 2019). In the food processing field, this technology allows printing of edible materials with customized 3D shapes, decoration, or even of the nutrient content of a meal. Some printed products might be further cooked using conventional methods or equipment, such as cooktops, stoves, and microwaves, or using advanced method, such as laser cooking (Blutinger et al., 2021; Blutinger et al., 2023). The ingredients used in food printing can be in several forms including powder, glutinous liquid, or molten material at room temperature (Wang et al., 2018). To date, many types of ingredients have been investigated, including starch (Thangalakshmi and Arora, 2021), chocolate (Mantihal et al., 2019), plant fiber (Pant et al., 2021), potato puree (Mirazimi et al., 2022), beef (Park et al., 2023), and soy protein isolate (Chen et al., 2019). The shaping techniques used on these ingredients include extrusion, selective laser sintering, binder jetting, and inkjet (Lv et al., 2023). Typically, the shaping technique of each ingredient is considered according to the desired effects of the printed food (Varvara et al., 2021).

Among these four mentioned techniques, extrusion-based printing is the most extensively used because of its simple processes and relatively low cost. For the extrusion-based technique, flowability and viscoelasticity of the substrate are important factors in achieving accuracy and the desired mechanical properties of the product (Chang et al., 2014). These properties result from the composition of the ingredients and also food additives, such as agar, lecithin, glycerol, and alginate (Dankar et al., 2018). In addition, the process parameters of the 3D printing machine influence the shape and texture of the printed product (Guénard-Lampron et al., 2021). For example, the effect of the printing speed, the movement speed of the nozzle during substrate extrusion, and the nozzle size on the quality of the printed potato starch-

protein were studied with the oleogel content prepared by mixing sunflower seed oil and beeswax, where using too high a printing speed caused low dimensional accuracy of the printed product and irregular extrusion delivery (Shi et al., 2021). An appropriate nozzle size should be carefully considered to achieve smoothness and dimensional accuracy. If the nozzle size is too small or too large, unstable extrusion behavior may result (Yang et al., 2019). In addition, the printing speed affected the extrusion rate of the substrate. Thus, mismatching between these two process parameters may cause undesired amounts of the deposited substrate (Derossi et al., 2020). Nozzle height (the distance between the nozzle tip and the deposited top layer) is another process parameter that can influence the printing quality. Wang and Shaw (2005) recommended an equation to estimate the critical nozzle height ( $h_c$ ):  $h_c = V_d/v_n \cdot D_n$ , where  $V_d$  is the extrusion rate ( $\text{mm}^3/\text{s}$ ),  $v_n$  is the printing speed ( $\text{mm/s}$ ), and  $D_n$  is the nozzle size ( $\text{mm}$ ). However, the nozzle height might require adjustment for a particular application. For example, the nozzle height was set to be equal to the nozzle size to ensure that the substrate could be attached to the previous layer, under the assumption of no shrinking/swelling or expansion (Yang et al., 2018).

The current study investigated the possibility of applying 3DP technology to shape “Khanom Ar-Lua”, a well-known ancient Thai dessert (shown in Fig. 1) into unique 3D shapes. Khanom Ar-Lua was inspired by a Portuguese recipe that was introduced to Thai people by Maria Guyomar de Pina (known in Thai as “Thao Thong Kip Ma”) in the 17th century, Ayutthaya era (Spencer, 2022). Khanom Ar-Lua should have a sugar crust, a soft crumbed texture and the flavor of coconut milk (Jantathai et al., 2014). Traditionally, Thai desserts, including Khanom Ar-Lua, are hand-made, which is time consuming in the preparation of the ingredients, forming exquisite shapes, and further cooking using conventional heating methods, such as steaming, frying, or even sun drying. 3DP technology has been considered in helping to decrease the processing time in



**Fig. 1** Examples of Khanom Ar-Lua: (A) general (Bakery Lover, 2022); (B) rose (Sentangsedtee Online, 2022); (C) lotus (Anita, 2021)

the shaping step. The current study designed a new mechanical extrusion system for deposition of the substrate that was installed on an extrusion-based 3DP machine. The mechanical extrusion system was tested based on the original recipe for Khanom Ar-Lua to identify the suitable process parameters to achieve a controllable paste as the substrate.

## Materials and Methods

### Material preparation

Typically, the main ingredients of Khanom Ar-Lua consist of wheat flour, white sugar, and coconut milk. In this study, the composition was based on the following recipe for these three ingredients: one-third of a cup (50 g), one and one-half cups (300 g), and one-half a cup (120 mL) respectively. In addition, food coloring was added to facilitate the dimensional controllability analysis. The printing substrate was prepared using the following steps: 1) dry mixing the sifted wheat flour and the white sugar in the mixing bowl; 2) blending gradually the coconut milk into the mixture; 3) stirring gently until the white sugar had dissolved completely; 4) removing any remaining lumps by sieving the mixture through a cheesecloth; 5) cooking the mixture using a non-stick pan on medium-low heat and stirring vigorously for 6 min (the stirring time varied depending on the heat setting of the stove) until the product was shiny, usually at 50°C; and 6) adding two drops of food coloring (pink) and stirring until the color of the substrate was homogeneous.

### Development of new mechanical extrusion system

Since the shaping process was carried out using an extrusion-based 3DP that was generally used for plastic filaments, a new mechanical extrusion system was designed and constructed to replace the original. The new system consisted of a nozzle, a barrel and a plunger. The nozzle (1.5 mm internal diameter) was installed on the X-Z axis of the 3DP. The barrel was installed on the gantry and its volume was 125 mL. The plunger was inserted into the barrel after filling with the substrate. Extrusion of the substrate was driven by a stepper motor (torque 45 N.cm, 1.7 A) and a transmission module containing two 36-toothed spur gears and a lead screw. Fig. 2 presents the new mechanical extrusion system on the 3DP.

### 3D printing machine

The 3DP machine had three main components: 1) an X-Y-Z positioning system driven by stepper motors, where the Y axis was used as a printing bed, while the X and Z axes were used for the printing head; (2) the printing bed; and 3) the mechanical extrusion system for printing the substrate. A Repitier host program (Hot-World GmbH & Co., Germany) was used to control the printing machine and to prepare the 3D models for printing.

### Process parameter identification

The developed mechanical extrusion system was tested for its setup suitability. For the extrusion based 3DP, high dimensional controllability is required when depositing the substrate on the platform or on top of the previous layer. This characteristic is vital for most Thai desserts because their shapes are quite exquisite and an essential part of the product. An experiment was conducted to determine a suitable extrusion rate for the developed mechanical extrusion system to provide the controllable dimensions of the deposited substrate. Typically, the extrusion rate is affected by printing speed as well as nozzle height. Inappropriate process parameters might cause printing problems, including flooding of the substrate, inconsistency of the deposited substrate and misalignment of the consecutive layers. In the current study, the printing speed and nozzle height were controlled at 6.5 mm/s and 10 mm, respectively. Based on the initial setup, a tentative range was investigated for a suitable extrusion rate. The results illustrated that using an extrusion rate lower than 5.3 mm<sup>3</sup>/s resulted in the substrate not being completely deposited on the platform. Furthermore, using an extrusion rate higher than 12.4 mm<sup>3</sup>/s at this printing speed deposited too much substrate on the platform with controllable dimension, resulting in

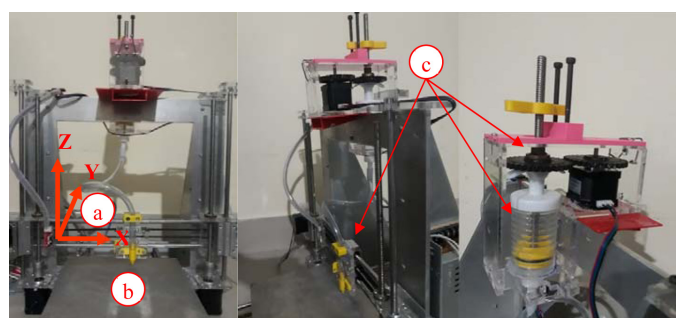


**Fig. 2** 3D printer equipped with new mechanical extrusion system: (a) X-Y-Z positioning system; (b) printing bed; (c) nozzle/barrel/plunger

unacceptable flooding. Therefore, the extrusion rate was varied using three levels ( $5.3 \text{ mm}^3/\text{s}$ ,  $8.8 \text{ mm}^3/\text{s}$  and  $12.4 \text{ mm}^3/\text{s}$ ) to avoid the above problems. Line tests were adopted to examine consistency and repeatability of the printed results to assess the dimensional characteristics of the deposited substrate. For each extrusion rate, 10 replications of a square ( $60 \text{ mm} \times 60 \text{ mm}$ ) were generated. Raster widths of the lines, in the X and Y directions, were measured at three positions: a midpoint and two positions close to the corners, as shown in Fig. 3. The other process parameters controlled were the nozzle diameter at 1.5 mm and the layer thickness at 1.5 mm.

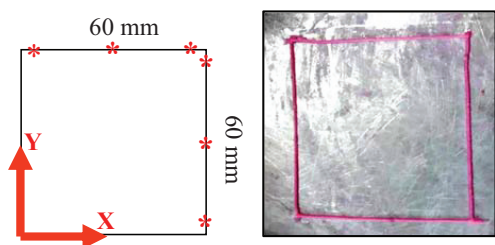


Fig. 3 Test positions of generated square

#### Statistical analysis of dimensional controllability

The dimensional controllability was assessed based on the consistency and repeatability of the deposited substrate. During the printing process, the deposited substrate should have low deviation of the raster width along the printing path as well as the raster width being reproducible.

As illustrated in Fig. 4, good consistency of the deposited substrate can be indicated from the standard deviation of

the raster width measured from three positions ( $SD_p$ ) that should each have a value of ideally zero or close to zero in practice. In addition, the average raster width of each testing line ( $\mu_p$ ) on both the X and Y axes should be conformed. A two-sample t test, under the assumption of equal variances, was conducted at the 95% confidence level ( $\alpha = 0.05$ ) to investigate the printing results obtained from different axes, i.e., whether the average raster width for the X axis ( $\mu_{px}$ ) was significantly different to the average raster width for the Y axis ( $\mu_{py}$ ), by posing two hypotheses ( $H_0 : \mu_{px} - \mu_{py} = 0$  and  $H_1 : \mu_{px} - \mu_{py} \neq 0$ ).

For each testing condition, good repeatability of the deposited substrate was indicated by the standard deviation of the average raster width of each testing line ( $SD_c$ ). The value of  $SD_c$  should be ideally zero or close to zero in practice, as shown in Fig. 4.

#### Results and Discussion

All specimens were generated and investigated for their raster widths. Table 1 shows the obtained results. For each replication, the raster width was measured at three different positions to determine their standard deviation ( $SD_p$ ). From the experimental results, the standard deviations of all replications were in the range 0.0058–0.0208 mm. Therefore, the consistency of the raster width was considered acceptable. This illustrated the performance of the developed mechanical extrusion system to provide the substrate while the printing nozzle was travelling along both the X and Y axes. The results obtained from different axes were analyzed with the two-sample t test. Table 2 shows the statistical results [ $p(T \leq t)$  two-tailed  $> \alpha$ ]; thus, there was no significant difference between the results obtained from the X and Y axes. At each extrusion rate, the repeatability was assessed by the standard deviation of the average raster width of 10 replications ( $SD_c$ ), as shown in Table 1. The lower the standard deviation, the higher the repeatability. Typically, commercial extrusion-based 3DPs, such as the Fused Deposition Modelling system, provide dimensional deviation at the micro level (Nuñez et al., 2015). The current testing resulted in standard deviations in the range 0.0031–0.0076 mm, which were considered to be quite low. These results illustrated good repeatability of the raster widths. The results obtained from the line tests illustrated that the mechanical extrusion system could provide good dimensional controllability.

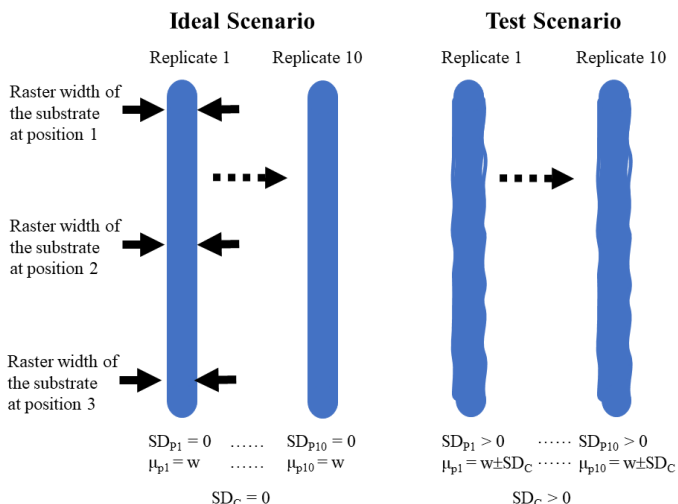


Fig. 4 Dimensional controllability analysis

**Table 1** Raster width analysis for different extrusion rates

Replicate	Extrusion rate (mm <sup>3</sup> /s)	Raster width of substrate in X-axis (mm)					Raster width of substrate in Y-axis (mm)				
		Position 1	Position 2	Position 3	$\mu_{px}$	SD <sub>px</sub>	Position 1	Position 2	Position 3	$\mu_{py}$	SD <sub>py</sub>
1	5.3	1.44	1.44	1.43	1.44	0.0058	1.43	1.44	1.43	1.43	0.0058
2		1.45	1.46	1.45	1.45	0.0058	1.44	1.46	1.45	1.45	0.0100
3		1.45	1.45	1.44	1.45	0.0058	1.45	1.45	1.44	1.45	0.0058
4		1.44	1.44	1.43	1.44	0.0058	1.44	1.44	1.43	1.44	0.0058
5		1.43	1.44	1.44	1.44	0.0058	1.43	1.44	1.43	1.43	0.0058
6		1.44	1.45	1.44	1.44	0.0058	1.44	1.45	1.44	1.44	0.0058
7		1.44	1.45	1.45	1.45	0.0058	1.43	1.45	1.44	1.44	0.0100
8		1.43	1.45	1.44	1.44	0.0100	1.44	1.45	1.43	1.44	0.0100
9		1.43	1.44	1.43	1.43	0.0058	1.44	1.44	1.43	1.44	0.0058
10		1.44	1.44	1.43	1.44	0.0058	1.43	1.44	1.44	1.44	0.0058
		$\mu_{cx}$					$\mu_{cy}$				
		1.4410					1.4397				
		SD <sub>ex</sub>					SD <sub>ey</sub>				
1	8.8	1.49	1.51	1.50	1.50	0.0100	1.50	1.52	1.51	1.51	0.0100
2		1.50	1.51	1.49	1.50	0.0100	1.51	1.52	1.50	1.51	0.0100
3		1.50	1.52	1.51	1.51	0.0100	1.50	1.52	1.51	1.51	0.0100
4		1.49	1.52	1.52	1.51	0.0173	1.49	1.53	1.52	1.51	0.0208
5		1.51	1.53	1.52	1.52	0.0100	1.51	1.52	1.51	1.51	0.0058
6		1.50	1.52	1.51	1.51	0.0100	1.50	1.52	1.51	1.51	0.0100
7		1.50	1.52	1.51	1.51	0.0100	1.50	1.51	1.50	1.50	0.0058
8		1.51	1.52	1.50	1.51	0.0100	1.51	1.52	1.50	1.51	0.0100
9		1.51	1.53	1.53	1.52	0.0115	1.51	1.52	1.51	1.51	0.0058
10		1.50	1.52	1.49	1.50	0.0153	1.50	1.53	1.51	1.51	0.0153
		$\mu_{cx}$					$\mu_{cy}$				
		1.5097					1.5107				
		SD <sub>ex</sub>					SD <sub>ey</sub>				
1	12.4	1.58	1.60	1.59	1.59	0.0100	1.57	1.59	1.59	1.58	0.0115
2		1.57	1.59	1.58	1.58	0.0100	1.58	1.60	1.60	1.59	0.0115
3		1.58	1.59	1.59	1.59	0.0058	1.58	1.59	1.59	1.59	0.0058
4		1.59	1.60	1.58	1.59	0.0100	1.57	1.60	1.59	1.59	0.0153
5		1.57	1.59	1.58	1.58	0.0100	1.59	1.59	1.58	1.59	0.0058
6		1.58	1.60	1.59	1.59	0.0100	1.58	1.60	1.60	1.59	0.0115
7		1.58	1.59	1.59	1.59	0.0058	1.59	1.59	1.58	1.59	0.0058
8		1.59	1.60	1.59	1.59	0.0058	1.58	1.60	1.59	1.59	0.0100
9		1.57	1.58	1.58	1.58	0.0058	1.59	1.60	1.58	1.59	0.0100
10		1.59	1.60	1.59	1.59	0.0058	1.57	1.59	1.59	1.58	0.0115
		$\mu_{cx}$					$\mu_{cy}$				
		1.5867					1.5880				
		SD <sub>ex</sub>					SD <sub>ey</sub>				

$\mu_{cx}$  = the average raster width on each test condition in the X axis;

SD<sub>ex</sub> = the standard deviation of the average raster width of each testing line in the X axis;

$\mu_{cy}$  = the average raster width on each test condition in the Y axis;

SD<sub>ey</sub> = the standard deviation of the average raster width of each testing line in the Y axis.

**Table 2** Results of the two-sample t test analysis

Extrusion rate (mm <sup>3</sup> /s)	5.3		8.8		12.4	
Axis	x	y	x	y	x	y
Mean	1.4410	1.4397	1.5097	1.5107	1.5867	1.5880
Variance	3.9630×10 <sup>-05</sup>	3.0741×10 <sup>-05</sup>	5.7901×10 <sup>-05</sup>	9.3827×10 <sup>-06</sup>	3.4568×10 <sup>-05</sup>	1.2840×10 <sup>-05</sup>
Number of observations	10	10	10	10	10	10
Pooled variance	3.5185×10 <sup>-05</sup>		3.3642×10 <sup>-05</sup>		2.3704×10 <sup>-05</sup>	
Hypothesized mean difference	0		0		0	
Degrees of freedom	18		18		18	
t Statistic	0.5026		-0.3855		-0.6124	
P(T<=t) two-tailed	0.6213		0.7044		0.5480	
t Critical two-tailed	2.1009		2.1009		2.1009	

The characteristics of the stacked layers were further investigated to consider if the process was suitable for use in real applications. The upcoming substrate should be deposited on top of the previous deposited substrate with accurate positioning. Two cylindrical workpieces (diameter 20 mm) were generated, with one having a height of 5 layers and the other a height of 10 layers. Fig. 5A shows the toolpath generated by the Repetier host program. Since the average raster widths obtained from each extrusion rate were quite close, a one-way analysis of variance was conducted based on the 95% confidence level ( $\alpha = 0.05$ ) to determine the effect of the extrusion rate on the average raster width of each testing line ( $\mu_p$ ). The results illustrated that there was a significant difference between the levels of the extrusion rate ( $F > F_{\text{crit}}$  or  $p\text{-value} (0.0000) < \alpha$ ), as shown in Table 3. Among the three levels of extrusion rate, 8.8 mm<sup>3</sup>/s produced an intermediate raster width (1.51 mm) that was considered for further investigation. Fig. 5B shows the substrate extruded through the nozzle with the extrusion rate of 8.8 mm<sup>3</sup>/s. Figs. 5C and 5D show the printed 3D workpieces with 5 layers and 10 layers, respectively. Clearly, there was some misalignment between the layers, which might have resulted from inappropriate ingredients in the substrate or the nozzle height being too high. This study aimed to present an alternative process to shape an ancient Thai dessert. Therefore, the ingredients should be maintained as in the original recipe or only minimally adjusted to preserve the original taste. The nozzle height was initially set at 10 mm to avoid flooding of the substrate over the space between the nozzle tip and printing bed. From initial tests with the original ingredients of Khanom Ar-Lua, the printing results tended to be uncontrolled and produced flooding. The nozzle height was set at 0.54–1.27 mm reported as the critical nozzle height by

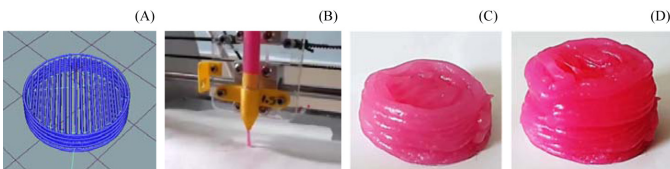


**Fig. 5** 3D workpieces: (A) toolpath; (B) extrudate; (C) 5-layered workpiece; (D) 10-layered workpiece

Wang and Shaw (2005) and at 1.5 mm, which was equal to the nozzle diameter, according to Yang et al. (2018). Although future work will be more focused on identifying the suitable nozzle height, the ingredient of the substrate might be revisited for minor adjustment in order to lower the nozzle height to improve the misalignment problem. As this factor has an influence on flow characteristics, such as viscosity and viscoelasticity (Wilms et al., 2021), changing the extrusion rate might allow the nozzle height to be optimized more effectively.

In addition, the processing time of the entire cooking process of Khanom Ar-Lua was considered. The printing times of the cylindrical workpieces were 83 s for the 5-layered height and 136 s for the 10-layered height. Both printed parts were air-dried using direct exposure to sunlight for 1 d to allow the skin to solidify sufficiently to allow each printed piece to be picked up without deforming, as shown in Fig. 5C and 5D. The moisture content of the parts was reduced to 40–50%. Subsequently, they were air-dried again for 1–2 d to improve their texture before eating. A lower moisture content results in a soft crumb texture, being a little hard outside with a dry skin but soft, moist and tender inside. Their shapes were unchanged but the skin color slightly faded after drying. Even though a hot-air oven could reduce the drying time, it would still be in the range 0.5–2 d, according to the drying conditions. Thus, a new drying method should be explored to improve the entire processing time of Khanom Ar-Lua and other Thai desserts that need heating following the initial cooking. A concept of precision cooking via multi-wavelength lasers was introduced for simultaneously cooking printed food (Blutinger et al., 2021), with the printing and cooking processes carried out using the same machine. A laser was applied immediately to the printed food after shaping a layer. This method could be considered for further development of Thai dessert printing.

Based on the results from this preliminary study, 3DP technology showed potential for application in the Thai dessert industry. Using the conventional process, ancient Thai desserts require considerable human effort and time to prepare the ingredients. In addition, some desserts need a lot of time to form their exquisite shapes, so that Thai dessert cooking

**Table 3** Results of the one-way analysis of variance

Source of variation	SS	df	MS	F value	p value	F critical value
Extrusion rate	0.216269	2	0.108135	3650.745	$6.9 \times 10^{-5}$	3.158843
Error	0.001688	57	$2.96 \times 10^{-5}$			
Total	0.217958	59				

SS = Sum of Squares; df = degrees of freedom; MS = Mean squares

has been described as an art (Kamonsinmahat, 2002). In an attempt to preserve ancient Thai desserts, their shapes should be digitally recorded using a 3D scanner and reverse engineering technology. Geometrical modelling of the Thai desserts is too difficult to be performed using a computer-aided design package because the dessert shapes are irregular. Point clouds could be processed into a digital record that could be physically fabricated and duplicated using 3DP.

## Conclusion

3DP technology was explored for its potential application in the Thai dessert industry, to replace the traditional handmade process. The process involved preparing and cooking the ingredients, forming the exquisite shape and then further heating, which all required a lot of time and intensive skills. An alternative cooking process was presented in this study. The developed extrusion-based 3DP was applied for shaping Khanom Ar-Lua, a well-known ancient Thai dessert. A new mechanical extrusion system was constructed and tested for dimensional controllability. Under the control of the original ingredients of Khanom Ar-Lua and the initial set of process parameters, the results showed potential for the developed system using this application as the raster width of the printed substrate to produce good consistency and repeatability. However, there was clearly a problem of the misalignment of consecutive layers due to an inappropriate nozzle height and a limitation relating to the long drying time after the shaping step that might not be realistic in commercial applications. Therefore, future studies should investigate: 1) identifying a suitable nozzle height to reduce the misalignment problem; and 2) improving the drying method to shorten the entire production time.

## Conflict of Interest

The authors declare that there are no conflicts of interest.

## References

Anita. 2021. Class Ar-Lua Bua-Sawan. <http://www.anitakanomthai.com/index.php/8-anitakanomthai/5-by-anita>, 16 June 2023. [in Thai]

Bakery Lover. 2022. Khanom Ar-Lua Krob-noak Num-nai. <https://kasetsart/DkTDOj>, 16 June 2023. [in Thai]

Blutinger, J.D., Cooper, C.C., Karthik, S., et al. 2023. The future of software-controlled cooking. *Npj Sci. Food.* 7: 6. doi.org/10.1038/s41538-023-00182-6

Blutinger, J.D., Tsai, A., Storwick, E., et al. 2021. Precision cooking for printed foods via multiwavelength lasers. *Npj Sci. Food.* 5: 24. doi.org/10.1038/s41538-021-00107-1

Chang, Y.Y., Li, D., Wang, L.J., Bi, C.-h., Adhikari, B. 2014. Effect of gums on the rheological characteristics and microstructure of acid-induced SPI-gum mixed gels. *Carbohydr. Polym.* 108: 183–191. doi.org/10.1016/j.carbpol.2014.02.089

Chen, J., Mu, T., Goffin, D., Blecker, C., Richard, G., Richel, A., Haubruege, E. 2019. Application of soy protein isolate and hydrocolloids based mixtures as promising food material in 3D food printing. *J. Food Eng.* 261: 76–86. doi.org/10.1016/j.jfoodeng.2019.03.016

Dankar, I., Pujolà, M., El Omar, F., Sepulcre, F., Haddarah, A. 2018. Impact of mechanical and microstructural properties of potato puree-food additive complexes on extrusion-based 3D printing. *Food Bioprocess Technol.* 11: 2021–2031. doi.org/10.1007/s11947-018-2159-5

Derossi, A., Paolillo, M., Caporizzi, R., Severini, C. 2020. Extending the 3D food printing tests at high speed. Material deposition and effect of non-printing movements on the final quality of printed structures. *J. Food Eng.* 275: 109865. doi.org/10.1016/j.jfoodeng.2019.109865

El-Sayegh, S., Romdhane, L., Manjikian, S. 2020. A critical review of 3D printing in construction: Benefits, challenges, and risks. *Arch. Civ. Mech. Eng.* 20: 34. doi.org/10.1007/s43452-020-00038-w

Guénard-Lampron, V., Masson, M., Leichtnam, O., Blumenthal, D. 2021. Impact of 3D printing and post-processing parameters on shape, texture and microstructure of carrot appetizer cake. *Innovative Food Sci. Emerg. Technol.* 72: 102738. doi.org/10.1016/j.ifset.2021.102738

Jantathai, S., Sungsri-In, M., Mukprasirt, A., Duerrschmid, K. 2014. Sensory expectations and perceptions of Austrian and Thai consumers: A case study with six colored Thai desserts. *Food Res. Int.* 64: 65–73. doi.org/10.1016/j.foodres.2014.06.007

Joshi, S.C., Sheikh, A.A. 2015. 3D printing in aerospace and its long-term sustainability. *Virtual Phys. Prototyp.* 10: 175–185. doi.org/10.1080/17452759.2015.1111519

Kamonsinmahat, P. 2022. Nine auspicious Thai desserts. [https://www.thailandfoundation.or.th/th/culture\\_heritage/nine-auspicious-thai-desserts/](https://www.thailandfoundation.or.th/th/culture_heritage/nine-auspicious-thai-desserts/), 11 July 2023.

Liaw, C.-Y., Guvendiren, M. 2017. Current and emerging applications of 3D printing in medicine. *Biofabrication* 9: 024102. doi: 10.1088/1758-5090/aa7279

Lv, Y., Lv, W., Li, G., Zhong, Y. 2023. The research progress of physical regulation techniques in 3D food printing. *Trends Food Sci. Technol.* 133: 231–243. doi.org/10.1016/j.tifs.2023.02.004

Mantihal, S., Prakash, S., Bhandari, B. 2019. Textural modification of 3D printed dark chocolate by varying internal infill structure. *Food Res. Int.* 121: 648–657. doi.org/10.1016/j.foodres.2018.12.034

Mirazimi, F., Saldo, J., Sepulcre, F., Gracia, A., Pujola, M. 2022. Enriched puree potato with soy protein for dysphagia patients by using 3D printing. *Food Front.* 3: 706–715. doi.org/10.1002/ff.2149

Nachal, N., Moses, J.A., Karthik, P., Anandharamakrishnan, C. 2019. Applications of 3D printing in food processing. *Food Eng. Rev.* 11: 123–141. doi.org/10.1007/s12393-019-09199-8

Nuñez, P.J., Rivas, A., García-Plaza, E., Beamud, E., Sanz-Lobera, A. 2015. Dimensional and surface texture characterization in fused deposition modelling (FDM) with ABS plus. *Procedia Eng.* 132: 856–863. doi.org/10.1016/j.proeng.2015.12.570

Pant, A., Lee, A.Y., Karyappa, R., et al. 2021. 3D food printing of fresh vegetables using food hydrocolloids for dysphagic patients. *Food Hydrocoll.* 114: 106546. doi.org/10.1016/j.foodhyd.2020.106546

Park, J.W., Lee, S.H., Kim, H.W., Park, H.J. 2023. Application of extrusion-based 3D food printing to regulate marbling patterns of restructured beef steak. *Meat Sci.* 202: 109203. doi.org/10.1016/j.meatsci.2023.109203

Park, Y.-G., Yun, I., Chung, W.G., Park, W., Lee, D.H., Park, J.-U. 2022. High-resolution 3D printing for electronics. *Adv. Sci.* 9: 2104623. doi.org/10.1002/advs.202104623

Sentangsedtee Online. 2022. Edible art, French Rose Ar-Lua. [https://www.sentangsedtee.com/food-recipes-for-job/article\\_181144](https://www.sentangsedtee.com/food-recipes-for-job/article_181144), 16 June 2023. [in Thai]

Shi, Y., Zhang, M., Bhandari, B. 2021. Effect of addition of beeswax based oleogel on 3D printing of potato starch-protein system. *Food Struct.* 27: 100176. doi.org/10.1016/j.foostr.2021.100176

Spencer, L. 2022. Maria Guyomar de Pinha, the Luso-Asian who introduced Portuguese desserts to Thai royalty. The Portuguese in Asia. <https://www.portuguese.asia/post/maria-guyomar-de-pinha-the-luso-asian-who-introduced-portuguese-desserts-to-thai-royalty>, 16 June 2023.

Tan, K.J., Hou, B., Ng, Y.H.J., et al. 2022. Implementation of additive manufacturing technologies in the design and build process of a two-seater high-performance electric vehicle. *Mater. Today Proc.* 70: 649–654. doi.org/10.1016/j.matpr.2022.10.033

Thangalakshmi, S., Arora, V.K. 2021. Assessment of rice flour and jaggery as a potential 3D food printer cartridge. In: Kumar, N., Tibor, S., Sindhvani, R., Lee, J., Srivastava, P. (Eds.). *Advances in Interdisciplinary Engineering: Lecture Notes in Mechanical Engineering*. Springer. Singapore, pp. 487–498. doi.org/10.1007/978-981-15-9956-9\_49

Vanderploeg, A., Lee, S.-E., Mamp, M. 2017. The application of 3D printing technology in the fashion industry. *Int. J. Fash. Des. Technol. Educ.* 10: 170–179. doi.org/10.1080/17543266.2016.1223355

Varvara, R.-A., Szabo, K., Vodnar, D.C. 2021. 3D food printing: Principles of obtaining digitally-designed nourishment. *Nutrients* 13: 3617. doi.org/10.3390/nu13103617

Wang, J., Shaw, L.L. 2005. Rheological and extrusion behavior of dental porcelain slurries for rapid prototyping applications. *Mater. Sci. Eng. A* 397: 314–321. doi.org/10.1016/j.msea.2005.02.045

Wang, L., Zhang, M., Bhandari, B., Yang, C. 2018. Investigation on fish surimi gel as promising food material for 3D printing. *J. Food Eng.* 220: 101–108. doi.org/10.1016/j.jfoodeng.2017.02.029

Wilms, P., Daffner, K., Kern, C., Gras, S.L., Schutyser, M.A.I., Kohlus, R. 2021. Formulation engineering of food systems for 3D-printing applications—A review. *Food Res. Int.* 148: 110585. doi.org/10.1016/j.foodres.2021.110585

Yang, F., Zhang, M., Bhandari, B., Liu, Y. 2018. Investigation on lemon juice gel as food material for 3D printing and optimization of printing parameters. *LWT* 87: 67–76. doi.org/10.1016/j.lwt.2017.08.054

Yang F., Zhang, M., Liu, Y. 2019. Effect of post-treatment microwave vacuum drying on the quality of 3D-printed mango juice gel. *Drying Technol.* 37: 1757–1765. doi.org/10.1080/07373937.2018.1536884

Yap, Y.L., Yeong, W.Y. 2014. Additive manufacture of fashion and jewellery products: A mini review. *Virtual Phys. Prototyp.* 9: 195–201. doi.org/10.1080/17452759.2014.938993